

Transport gap in a $\nu=1/3$ quantum Hall system: A probe for skyrmions

Annelene F. Dethlefsen* and Rolf J. Haug

Institut für Festkörperphysik, Universität Hannover, Appelstraße 2, D-30167 Hannover, Germany

Karel Výborný and Ondřej Čertík

*Fyzikální ústav, Akademie věd České republiky, Cukrovarnická 10, CZ-16253 Praha 6, Czech Republic
and 1. Institut für theoretische Physik, Universität Hamburg, Jungiusstrasse 9, D-22305 Hamburg, Germany*

Arkadiusz Wójs

*Institute of Physics, Wrocław University of Technology, Wybrzeże Wyspiańskiego 27, 50-370 Wrocław, Poland
(Received 17 March 2006; revised manuscript received 19 July 2006; published 14 November 2006)*

Transport measurements of the activation gap at fractional filling factor $1/3$ are compared to results of exact diagonalization, allowing identification of a small anti-skyrmion as the lowest excitation in the low-field regime. In agreement with theory, a crossover to spinless excitations at higher electron densities is observed. Two samples of different quality are investigated. A detailed description of the theoretical calculation of activation gaps is presented and features which should be taken into account are summarized: finite thickness, Landau level mixing, and comparison between different sizes of the model system and—whenever possible—also between different geometries (torus and sphere). Within the chosen model of disorder (entailing a single fit parameter) we obtain a good agreement between calculated energies and experimental results.

DOI: [10.1103/PhysRevB.74.195324](https://doi.org/10.1103/PhysRevB.74.195324)

PACS number(s): 73.43.Lp, 75.10.Jm, 72.10.Fk

I. INTRODUCTION

The existence of skyrmions is one of the remarkable many-body phenomena accompanying the quantum Hall effects. After the existence of skyrmions was established^{1–4} in the integer quantum Hall effect (IQHE) the question appeared whether they can also be observed in the regime of the fractional quantum Hall effect (FQHE), given the composite fermion (CF) mapping between the IQHE and the FQHE.⁵ We report here on an experiment indicating that the answer is positive.

A skyrmion can be viewed as a finite-size quasiparticle of charge $e < 0$ located at r_0 in the parent ground state, which is, e.g., the fully polarized (\uparrow) completely filled lowest Landau level (LL). More precisely, it is the many-body ground state at magnetic field B corresponding to the filling factor $\nu = (n_e h / |e| B) = 1$ minus one magnetic flux quantum (n_e is the electron density, h Planck's constant, and e the elementary charge of an electron). In this state, called also a spin texture, the expectation value of the spin is reversed (\downarrow) at $r = r_0$, it remains unchanged (\uparrow) for $r \rightarrow \infty$, and it interpolates smoothly between r_0 and infinity.⁶ A size K (precise definition in Sec. III) can be attributed to a skyrmion, related to how fast the spin changes with displacement from the skyrmion center. For magnetic fields of $\nu = 1$ plus one magnetic flux quantum, a symmetric quasiparticle of charge $-e$ exists, an anti-skyrmion.

Skyrmions at integer filling factors can be studied either using Hartree-Fock⁶ and field theoretic methods^{7–9} on one side or by exact diagonalization^{10–12} on the other side and all these approaches are interrelated.¹³ The central conclusion is that while the Zeeman energy favors small sizes K , meaning a small average number of reversed spins, the Coulomb (exchange) energy favors spatially smooth spin textures, i.e., large skyrmions, where two neighboring spins are almost

parallel. The size of the skyrmion lowest in energy is thus determined by the ratio of the Zeeman and Coulomb energies, $\eta = E_Z / E_C = \mu_B g B / [e^2 / (4\pi\epsilon\ell_0)] \propto \sqrt{B}$, where $\ell_0 = \sqrt{\hbar / |e| B}$ is the magnetic length, μ_B the Bohr magneton, g the effective electron Landé factor, and ϵ the dielectric constant. This conclusion remains valid also for integer filling factors¹⁴ $\nu > 1$, albeit the nonmonotonic Haldane pseudopotentials imply richer skyrmion phase diagrams.¹¹

Works related to fractional filling factors,^{7,11,15,16} most importantly to $\nu = 1/3$ which is the CF counterpart to $\nu = 1$ of electrons, lead to the same conclusion. However, apart from quantitative differences in skyrmion energies, fractional and integer systems showed some qualitative differences. The exact symmetry between skyrmions ($\nu > \frac{1}{3}$) and anti-skyrmions ($\nu < \frac{1}{3}$) is absent¹¹ and thus skyrmion and anti-skyrmion sizes need not be the same in one system. Also, the temperature dependences of the magnetization are different in the IQHE and FQHE regimes.^{17,18}

Experimentally, skyrmions were demonstrated in magnetotransport and in the Knight shift of NMR or magnetoabsorption spectroscopy sensitive to the spin polarization of the two-dimensional electron gas (2DEG). The first method probes skyrmion–anti-skyrmion pairs as an excitation on the background of the fully spin polarized (ferromagnetic) ground state at exactly $\nu = 1$. The other two methods probe the ground state at a slightly changed filling factor. Provided the filling factor is not too far from 1, the ground state remains the ferromagnetic state plus one skyrmion (anti-skyrmion) per magnetic flux removed (added) to the system. The depolarization in units of electron spin per one magnetic flux is thus equal to the average size of a skyrmion, i.e., to the number of involved spin flips.

From the transport activation gap at filling factor 1, Schmeller *et al.*² concluded that a typical excitation in a GaAs heterostructure contains seven spin flips. If the excita-

tion is a skyrmion-anti-skyrmion pair, each of these should have a size of $K=3$. The number of spin flips (size) was found to decrease with increasing ratio of Zeeman and Coulomb energies η . The optical experiments³ and the NMR experiments¹ gave approximately the same result. Hydrostatic pressure reduces the effective Landé g factor in GaAs and even $g=0$ is experimentally possible. It allows one to access smaller values of η compared to performing measurements at low magnetic fields where the QHE will eventually disappear. Maude *et al.*⁴ observed skyrmions as large as $K=16$ in magnetotransport at nearly vanishing Zeeman energy.

The Coulomb energy stabilizing skyrmions is much smaller at $\nu=\frac{1}{3}$ as compared to $\nu=1$. As a consequence, the skyrmions in the FQHE regime are usually smaller. Leadley *et al.*¹⁹ found excitations with three spin flips in magnetotransport at nearly $g=0$ implying skyrmion sizes (K_S) and anti-skyrmion sizes (K_A) with $K_A+K_S+1=3$. In contrast to this, NMR measurements by Khandelwal *et al.*²⁰ suggested $K_A \approx K_S \approx 0.1$. The reason for this very different result is unclear.

Experimental arguments in favor of skyrmions at $\nu=\frac{1}{3}$ are by far not so numerous as those for integer filling factors. Owing to our experiments, which agree well with exact diagonalization calculations, we believe the existence of skyrmions in the FQHE is confirmed, as well as the skyrmion-anti-skyrmion asymmetry, demonstrating the qualitative differences between electrons and composite fermions.

We present measurements of the $\nu=\frac{1}{3}$ activation gap Δ on two gated heterostructures of different mobilities as a function of the electron density n_e , i.e., the magnetic field B (Sec. II). We observe a rather linear $\Delta(B)$ behavior in a large region of magnetic fields implying that, roughly, the probed excitation costs much Zeeman energy and little Coulomb energy. In order to identify this spin excitation we analyze the measured $\Delta(B)$ (Sec. IV) and find that the lowest excitation in the high-mobility sample contains two spin flips while it has a single spin flip for the low-mobility sample. The Coulomb energy obtained during the analysis agrees reasonably with the theoretically calculated one of a pair of the smallest anti-skyrmion and a quasielectron with reversed spin (QEr) and, for the low-mobility sample, of a spin wave—a pair of a QEr and a quasihole (QH).

Moreover, we observe a clear transition to a different lowest excited state for $B \gtrsim 9$ T in the high-mobility sample. Again, an analysis of the measured $\Delta(B)$ was performed and it suggests that the relevant excitation contains no spin flip. This agrees with the usual statement that such excitations in the high- B limit belong to the magnetoroton (MR) branch at very large wave vector k . However, in the present case we observe a remarkable coincidence between the activation gap and the magnetoroton minimum, i.e., the MR at $k\ell_0 \approx 1.4$. We propose that this could be because the activation is a two-step process where creation of the bound magnetoroton is a bottleneck.

The exact diagonalization model used for theoretical calculations of Coulomb energies is described in Sec. III. Starting with ideal systems (ideally a 2D system, with no Landau level mixing) we summarize how activation gaps due to skyrmionic excitations can be calculated (Sec. III A). Next

TABLE I. Parameters of the investigated samples.

Sample	Spacer width (nm)	Density (m^{-2}) $T \approx 40$ mK, dark	Mobility ($\text{m}^2/\text{V s}$) $T \approx 40$ mK, dark
1	70	1.3×10^{15}	700
2	40	1.6×10^{15}	79

we focus on differences between ideal and realistic systems. We take into account the finite thickness of the 2D electron gas as well as the Landau level mixing (Sec. III B), which imply here only quantitative corrections to the energies calculated in ideal systems (Sec. III C). Modeling the disorder ubiquitous in real samples by a B -field-independent gap reduction,^{21,22} as the single fitting parameter (Sec. III B), the calculated Coulomb energies agree well with measured activation gaps.

II. THE EXPERIMENT

The investigated two-dimensional electron systems are realized in $\text{Al}_{0.33}\text{Ga}_{0.67}\text{As}/\text{GaAs}$ heterostructures. The sample growth parameters are given in Table I.

The basic difference between the samples is their mobility. The high quality of sample 1 allows the study of several different FQHE states, whereas the mobility below $100 \text{ m}^2/\text{V s}$ is sufficient only for studies of the most robust FQHE state, $\nu=1/3$, in sample 2.

A metallic top gate allows us to vary the electron density in a wide range. For sample 1 the electron density n_e is varied between 0.2×10^{15} and $1.3 \times 10^{15} \text{ m}^{-2}$ with a zero-field mobility reaching $700 \text{ m}^2/\text{V s}$ at 40 mK. With sample 2, densities between 0.59×10^{15} and $1.6 \times 10^{15} \text{ m}^{-2}$ can be accessed. Here the zero-field mobility reaches $79 \text{ m}^2/\text{V s}$ at 40 mK.

The experiments are performed in a dilution refrigerator with magnetic fields up to 20 T. The longitudinal resistivities ρ_{xx} (Shubnikov-de Haas oscillations) of the two samples at nearly the same electron densities are shown in Fig. 1, demonstrating the different quality of the samples. While the sample 2 exhibits only one minimum between filling factors $\nu=1$ and $1/3$, for sample 1 there is a series of different fractional quantum Hall states in this region.

To obtain the activation energy for the different magnetic fields we investigate the temperature dependence of the resistivity minimum at $\nu=1/3$. The temperatures in our experiment are varied between $T=40$ and 1000 mK. In this range the error of measurement of the calibrated ruthenium oxide sensor is ± 1 mK. We extract the gap Δ out of Arrhenius-plot data, using the activated resistance behavior $\rho_{xx} \propto \exp(-\Delta/2T)$. We assume that our total uncertainty in Δ is less than 2%. The measured activation energies Δ are shown in Fig. 2 for the two samples.

III. EXACT DIAGONALIZATION

Electron-electron interaction is the fundamental effect giving rise to most of the phenomena occurring within the lowest LL. Because of the extremely high degeneracy of

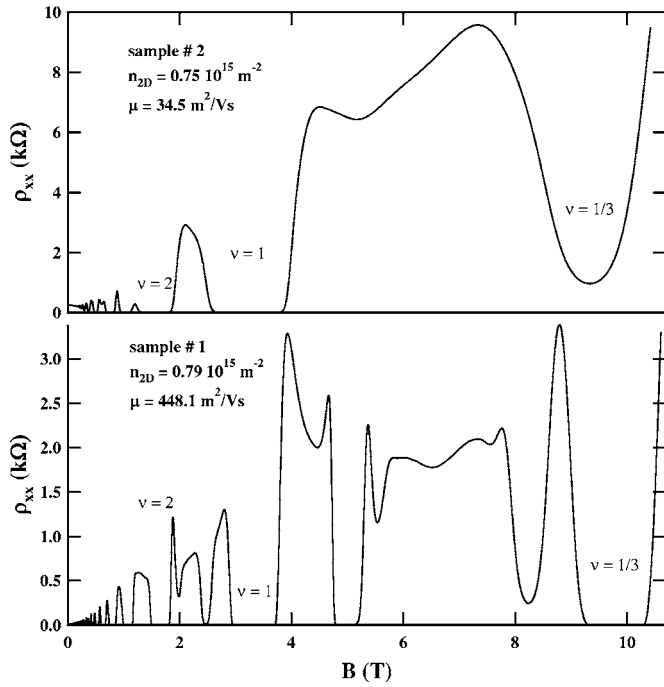


FIG. 1. Shubnikov–de Haas oscillations for both samples at similar electronic densities.

LLs, standard techniques like the Hartree-Fock approximation are inapplicable for describing these phenomena.

In the exact diagonalization (ED) approach,^{23,24} we start with the complete many-body Hamiltonian. It comprises the electron-electron interaction and the Zeeman energy,

$$H = \sum_{J, \Sigma} \mathcal{A}_J c_{j_1 \sigma_1}^\dagger c_{j_2 \sigma_2}^\dagger c_{j_3 \sigma_2} c_{j_4 \sigma_1} + \sum_{j, \sigma} E_Z \frac{\sigma}{2} c_{j \sigma}^\dagger c_{j \sigma},$$

$$J = (j_1, j_2, j_3, j_4), \quad \Sigma = (\sigma_1, \sigma_2). \quad (1)$$

Here j_i is the orbital quantum number, $\sigma = \pm 1$ is the spin, and $c_{j \sigma}^\dagger$ are the operators creating the corresponding one-electron

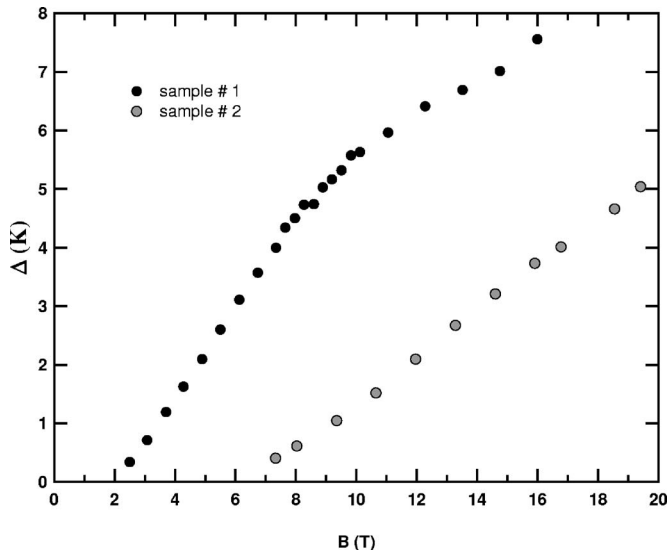


FIG. 2. Gap energies at $\nu=1/3$ from samples 1 and 2.

states. A convenient one-particle orbital quantum number is either the angular momentum or one component of the linear momentum. These choices are typical for spherical geometry and torus geometry, respectively. The last two notions describe the central approximation of the ED model. Instead of an infinite plane, we study a compact manifold preferably without edges, that is, we confine the electrons either to the surface of a sphere²⁵ or to a rectangle with periodic boundary conditions²⁶ (torus). The Coulomb matrix elements \mathcal{A}_J are given explicitly in Ref. 26 for the torus and they straightforwardly follow from the Haldane pseudopotentials on a sphere.²⁵ The Zeeman energy is just $E_Z = \mu_B g B$.

For the moment, we did not include any cyclotron energy ($\hbar\omega = \hbar e B / m^*$) term into (1). All electrons are assumed to stay in the lowest LL, which is true for the ground state and low-lying excited states if $\hbar\omega \gg \mathcal{A}_J, E_Z$ and $\nu \leq 2$. This approximation, exclusion of the LL mixing, is justified in the high- B limit because $\hbar\omega, E_Z \propto B$, $\mathcal{A}_J \propto \sqrt{B}$, and $\hbar\omega / E_Z \approx 60 \gg 1$.

The homogeneous magnetic field in the 2D system now corresponds to $N_m = 2Q$ quanta of magnetic flux passing through the surface of the sphere or torus. In this situation, exactly N_m one-electron states exist in the system.^{23,27} If we now put N electrons into the system, the filling factor is $\nu = N / N_m$ for the torus and $\nu = N / (N_m + \delta)$ for the sphere. The quantity δ is of the order of unity ($\delta / N_m \rightarrow 0$ for $N_m \rightarrow \infty$) and it is related to the topology of the considered eigenstate.²⁸

The number of all possible N -electron states is then finite. The matrix of the Hamiltonian (1) in this complete basis is evaluated and diagonalized, yielding the energies and many-body wave functions. An important feature of the Hamiltonian is that both the total spin S and z component are good quantum numbers. This fact is trivial for the Zeeman term and also for the first term in Eq. (1) since spin does not explicitly occur in it. The spin symmetry could be lifted, for instance, by magnetic impurities present in the system.

A. Activation energy in transport

It has been widely accepted that the activation gap Δ is the lowest energy needed to create a neutral pair of charged particles and to separate them very far from each other.^{29,30} Starting from the Laughlin ground state at $\nu = \frac{1}{3}$, these particles are not an electron and a hole. Rather they are particle-like many-body excitations³¹ with charge q and spin s (its component along the polarization direction of the $\nu = \frac{1}{3}$ state). They are usually called quasielectrons ($q = e/3, s = 1/2$) and quasiholes ($q = |e|/3, s = 1/2$), eventually with reversed spin ($q = e/3, s = -1/2$) as regarding to the direction preferred by the Zeeman energy. These quasiparticles will be denoted by QE, QH and QEr, respectively. The creation energies of all these three quasiparticles are different, even disregarding the Zeeman contribution, owing to their actual many-body nature. This is a fundamental difference from IQH systems.

Because of their charge $e/3$, all interactions between the mentioned quasiparticles at $\nu = 1/3$ (e.g., the skyrmion energies discussed below) are roughly weaker by an order of magnitude compared to $\nu = 1$. The interactions at long range are similar to the common Coulomb repulsion or attraction

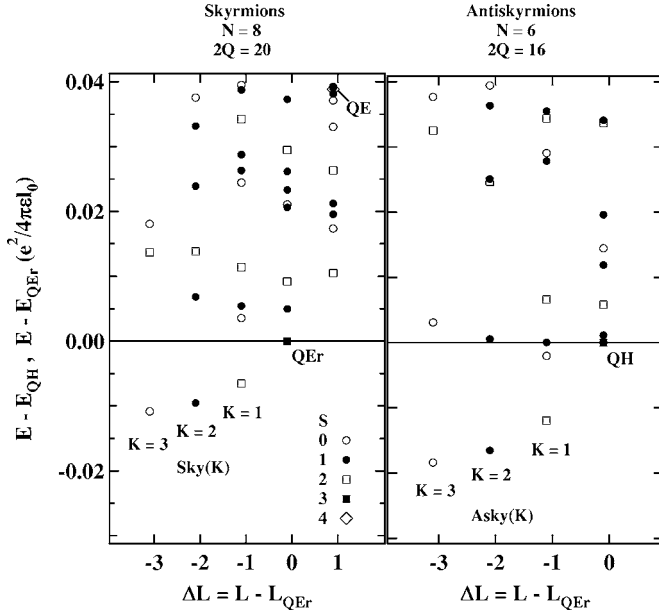


FIG. 3. Full skyrmion and anti-skyrmion spectra at $\nu=1/3$ minus and plus one magnetic flux quantum, respectively, and zero Zeeman energy. The (anti-)skyrmion branches of $\Delta L = -K$ have negative energy and they are well separated from the continuum of excited states. For $\nu > 1/3$, the quasielectron with reversed spin (QEr) is lower in energy than the QE. This holds for systems of all accessible sizes (here six and eight electrons).

because the size of the quasiparticles is of the order of ℓ_0 . At short range, on the other hand, it is not guaranteed that the interactions are similar to electrons because of the internal structure of the quasiparticles.^{32,33} Unlike the QE, the charge densities of QEr and QH are basically structureless and this fact lies at the heart of the close analogy between low-energy excitations at $\nu=1/3$ and 1.

The Coulomb energy of skyrmions and anti-skyrmions can be obtained from the ED spectra *on a sphere*³⁴ in a system with one flux quantum less and one flux quantum more, respectively, than what would correspond to $\nu = \frac{1}{3}$ (Fig. 3). For $E_Z \gg A_J$, the lowest excitation to determine the activated transport will involve creation of a QE+QH pair. As E_Z decreases, the lowest excitation becomes QEr+QH, because the energy of a QEr (Coulomb “correlation” energy) is lower¹¹ than the energy of a QE (Fig. 3, left). This will, however, not remain true in the limit $E_Z \rightarrow 0$. There are objects with even lower Coulomb energy than the QEr and QH. For each $K=1, 2, \dots$ there is one such object with total spin $K+1/2$ and charge $e/3$ and $-e/3$. These are usually called skyrmions (Sky) and anti-skyrmions (ASky), respectively. Contrary to IQH systems, the energies of the Sky(K) and ASky(K) are different, implying that the skyrmion size K_S and the anti-skyrmion size K_A need not be equal in the same system. Sky(K) [ASky(K)] is the energy difference between the QEr (QH) and the lowest state with angular momentum and spin

$$L = L_{\text{QEr,QH}} - K, \quad S = S_{\text{QEr,QH}} - K. \quad (2)$$

In a system of N electrons, the angular momenta used are $L_{\text{QH}} = S_{\text{QH}} = N/2$ and $L_{\text{QEr}} = S_{\text{QEr}} = N/2 - 1$. With this defini-

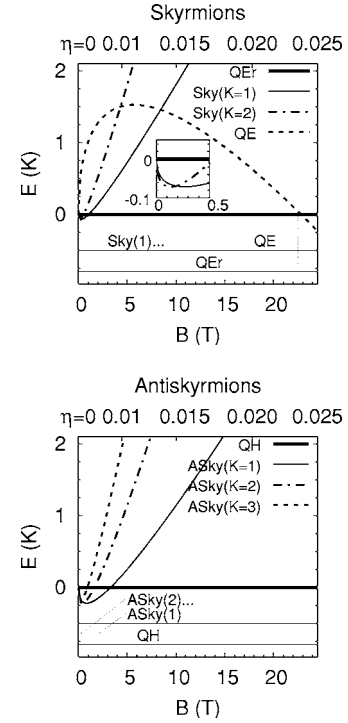


FIG. 4. Single skyrmion and anti-skyrmion energies at $\nu=1/3$ relative to the QEr and QH in an ideal system. More precisely, these are the ground-state energies at $\nu=1/3$ plus (minus) one flux quantum relative to the Laughlin state plus one QH (QEr), as indicated by the bars at the bottom of each graph. Energies obtained from the exact diagonalization were extrapolated to $1/N \rightarrow 0$.

tion, ASky(0) is a QH and Sky(0) is a QEr, meaning that ASky(K) contains K flipped spins while Sky(K) contains $K+1$ flipped spins. The states in Fig. 3 of lower energy than the QH can therefore be interpreted as quasiparticles ASky(K) of spin $S=K$ and $S_z=-K$ existing on the background of the polarized Laughlin liquid with $S=S_z=N/2$ [Eq. (2)].

Contrary to Eq. (2), the field theoretic models of skyrmions⁶⁻⁹ do not conserve L and S separately, but only $L+S$. Such states can be decomposed into those obtained by exact diagonalization as was shown by Rezayi.¹³ On the other hand, the exact Hamiltonian (1) does conserve all S , S_z , and L . Hence the number of spin flips involved in an excitation, or the size of a skyrmion, must always be an integer. Also note that we consider (small) finite-size skyrmions here, which can be modeled by exact diagonalization, while sometimes the term “skyrmion” is reserved for $K \rightarrow \infty$.

Figure 4 shows the competition between skyrmions of different sizes as a function of magnetic field, which means that the ratio between the Coulomb and Zeeman energies, η , is varied. The Zeeman energy favors small skyrmions since these include fewer spin flips. Thus, for fields above 3.2 T (1.0 T) no anti-skyrmions (skyrmions) occur in an ideal system as the Zeeman energy ($\propto B$) is then too large compared to the binding (Coulomb) energy ($\propto \sqrt{B}$). Owing to a rather high Coulomb energy cost, the QE becomes favored over the QEr first at rather high magnetic fields; Fig. 4 (left). It follows that skyrmions as well as anti-skyrmions with $K > 1$

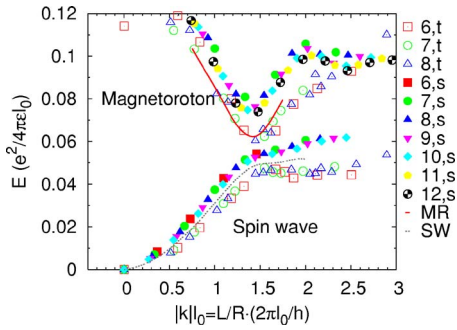


FIG. 5. (Color online) The spin wave (SW) and the magnetoroton branch (MR) seen in the ED spectra of ideal $\nu=1/3$ systems of different sizes and geometries. In the legend, t stands for torus, s for sphere, and the number indicates the number of electrons. The lines (solid and dotted) were obtained from the $1/N \rightarrow 0$ extrapolation of the data (MR and SW) on the sphere.

occur first at B as low as 1 T. These fields are far too low for the FQHE to be observed, so the only spin-flip excitations likely to be experimentally observed at $\nu=1/3$ are the QEr and ASky(1).

Once a neutral pair of quasiparticles Sky(K_S) and ASky(K_A) has been created, they behave similarly to a magnetoexciton. In a magnetic field, the magnetoexciton has a constant linear momentum k which is proportional to the mutual distance Δx between the quasiparticles. We would expect its energy to be $E(\Delta x) \propto 1/\Delta x$ with proportionality constant determined by the charges of the two constituent quasiparticles. Such modes can be calculated within the single-mode approximation³⁵ or starting with the Hamiltonian theory of composite fermions³⁶ but they can also be directly identified in the exact diagonalization spectra (Fig. 5). They are usually called the magnetoroton branch $E_{MR}(k)$ for QE+QH and the spin wave (SW) $E_{SW}(k)$ for QEr+QH. The limiting values for $k \rightarrow \infty$ are the energies necessary to create a QE+QH (QEr+QH) pair and to separate them far from each other. These are the quantities commonly used for comparison to the transport activation gaps, because the SW (MR) is the lowest excitation (at $k \geq 1.0\ell^{-1}$) among all states with total spin $S=N/2-1$ ($S=N/2$), i.e., with one (no) spin flip.

It is remarkable how much $E_{MR}(k)$ calculated on a sphere and on a torus differ, on a quantitative level (Fig. 5). Even though the positions of the magnetoroton minimum match well in both geometries ($k\ell_0 \approx 1.4$), the sphere gives seemingly a higher energy of the minimum by as much as 20%. A careful extrapolation to infinite systems (solid line in Fig. 5), however, matches excellently the results obtained on a torus. This is not surprising, given the magnetoexcitonic character of the MR. The MR of Δx comparable to the radius of the sphere will have the QE and the QH located near the opposite poles. This situation is not compatible with a picture of a plane wave of $k=\Delta x/\ell_0^2$ propagating along the equator. On the other hand, with increasing radius of the sphere R this becomes a finite-size effect if $R \gg \Delta x$. Based on Fig. 5, we believe finite-system data from the torus are more suitable to give quantitative estimates for magnetoroton and spin wave energies.

For a Sky(K_S)–ASky(K_A) pair, we take $E_{SW}(k)$ with $k \rightarrow \infty$ and add the creation energies of Sky(K_S) and of ASky(K_A). Instead of one system, as was the case for studying the QEr+QH pair, we thus have to exactly diagonalize three different systems: one for the quasiparticle-separation procedure, one for the Sky, and one for the ASky. This more complicated procedure suffers possibly less from finite-size effects, since skyrmions are rather extended objects, in particular more extended than a bare QH or QEr. Recall that the sizes of the Sky and ASky need not be the same.

B. Finite thickness, LL mixing, disorder

Aiming at the description of experiments under realistic conditions, three ever valid facts should not be left unnoticed: the sample is actually three dimensional (finite extent of the wave function perpendicular to the 2DEG), the magnetic field is finite (mixing between Landau levels), and the system is never perfectly homogeneous (disorder).

Nonzero thickness w of the 2DEG can be effectively incorporated into the Haldane pseudopotentials²⁵ which completely determine the Hamiltonian of the lowest LL. Qualitatively, the larger the effective thickness w/ℓ_0 , the more softened becomes the effective electron-electron interaction at the shortest distances.

Quantitative effects of the presence of the third dimension have been studied since the early times of the FQHE, both with the Laughlin state³⁷ and the activation gap.³⁸ In a heterostructure, electrons are confined to a nearly triangular potential well. A standard choice for the wave function in the growth direction is then the Fang-Howard trial wave function,³⁹ $\psi_{FH}(z) = (b^3/2)^{1/2} z e^{-bz/2}$. We will mostly stay with this choice, even though we are aware of other options for $\psi(z)$ which may lead to slightly lower subband energies (Sec. V in Morf *et al.*⁴⁰). Differences originating from these different choices of $\psi(z)$ should be smaller than the uncertainty in the variational parameter b (or the thickness of the 2DEG) relevant for our experiments. This has been checked with $\psi_{QW}(z) = \cos az$, $|z| < \pi/2a$, relevant for symmetric quantum wells. Taking $\psi_{FH}(z)$ instead of $\delta(z)$ is equivalent³⁸ to using a nontrivial form factor $F(q)$ in the 2D Fourier transforms $V(q)$ of the Coulomb interaction,

$$V(q) = \frac{F(q)}{q}, \quad F(q) = \frac{8 + 9(q/b) + 3(q/b)^2}{(2 + 2q/b)^3}. \quad (3)$$

The quantity $V(q)$ then enters the Coulomb matrix elements in (1) as given in standard references.^{23,41} These can be in turn reexpressed in terms of the Haldane pseudopotentials⁴² V_m . For reasonable values of b , only V_0 changes appreciably; it decreases by 25% for $b^{-1} = 0.3\ell_0$.

The spatial extent of the wave function along z defined as the full width at half maximum (FWHM) is $w \approx 4.9/b$ for ψ_{FH} and $w = \frac{2}{3}/a$ for ψ_{QW} . The wave function parameter b depends on the form (steepness) of the triangular well potential and therefore it is not constant but it changes with the applied gate voltage. This leads to^{38,39}

$$b = (33\pi m^* e^2 n_e / 2\varepsilon\hbar^2)^{1/3}, \quad (4)$$

which depends only on the electron density²³ n_e and the dielectric constant ε . If we assume the filling factor fixed at $1/3$, the density becomes a function of the magnetic field, so that

$$\beta = (b\ell_0)^{-1} \approx 0.23 \times [B(\text{T})]^{1/6}. \quad (5)$$

This is a formula relevant for both our samples. Thus, the parameter β varies between 0.27 and 0.38 in the experiments described herein.

The LL mixing is more difficult to include. If we admit that higher Landau levels may also be populated even at $\nu < 1$, we must (i) add the cyclotron energy term $\sum_{nj\sigma} (n + 1/2)\hbar\omega_c^\dagger c_n$ to the Hamiltonian (1). We also have to considerably extend the many-body basis (ii) because we have introduced a new single-particle orbital quantum number, the Landau level index n . The former fact also implies that we have a new energy scale proportional to B in the problem. Recall here the criterion for the neglect of LL mixing: $1 \gg A_j/\hbar\omega \propto 1/\sqrt{B}$. Fortunately, the magnetic fields relevant for the FQHE are still high enough for LL mixing to be treated perturbatively. In practice this means that in the first (second) order we allow for maximum one (two) particles to be in the first LL ($n=1$) when constructing the many-body basis. For the current purpose we allowed for up to two particles in the first Landau level and verified in small systems that increasing this number does not change the energies perceptibly.

Without higher LLs, the energies E_C of Hamiltonian's (1) Coulomb part were conveniently evaluated in the Coulomb units $e^2/(4\pi\varepsilon\ell_0)$. Then the energies were magnetic-field independent for $E_Z \equiv 0$ and depended via S_z trivially on B for $E_Z \neq 0$, in particular $E_Z/[e^2/(4\pi\varepsilon\ell_0)] \propto S_z\sqrt{B}$. With other LLs included in addition to the lowest one, $E_C/[e^2/(4\pi\varepsilon\ell_0)]$ becomes a function of B or better of⁴¹ $\lambda = \hbar\omega/[e^2/(4\pi\varepsilon\ell_0)]$. However, since variations of $E_C/[e^2/(4\pi\varepsilon\ell_0)]$ as a function of $B(\lambda)$ are typically small (see Fig. 6), we will adhere to the Coulomb units.

Disorder is to the best of our knowledge the only relevant effect not described microscopically within this work. A common notion is that the disorder reduces the incompressibility gap.⁴³ In fact, randomly distributed potential impurities included into the system (1) change the energies of both the ground state and the excited state. Because the excited states in question consist of two microscopic quasiparticles on the background of the Laughlin ground state, we will assume for our purposes that the disorder reduces the excitation energy by a constant.^{21,22,44} The reduction E_d was determined by fitting within the present work (see below, Sec. IV), and it is typically of the order of 1 K (cf. Fig. 9). Even though E_d depends primarily on the sample quality (larger mobility—smaller E_d), it is likely that it is also not the same for different excitations (skyrmions, magnetorotons) within a single sample. This fact renders any model calculations (without a very detailed microscopic theory of disorder) only capable of giving estimates, rather than exact values of B_c where crossovers between the two lowest excitations should occur. For instance, in order to determine the QEr-QE tran-

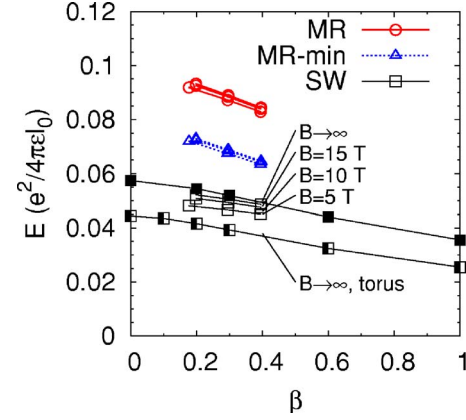


FIG. 6. (Color online) The effect of the finite thickness and the LL mixing on the magnetoroton (MR) minimum and on the best approximation to the $k \rightarrow \infty$ energies of the spin wave (SW) and the MR branch. A finite system (seven electrons) on a sphere is considered, except for the single curve marked “torus.” Energies labeled with B include the Landau level mixing which vanishes for $B \rightarrow \infty$.

sition properly (Fig. 4, left), we would have to shift the QE energies by a constant $E_d^{\text{QE}} - E_d^{\text{QEr}}$ downward thereby shifting the intercept of the QE and QEr curves considerably. However, this is not a major trouble as long as we study only one excitation (or several excitations separately).

C. Numerical data

The finite thickness of the 2DEG and the LL mixing do not change the SW and MR dispersions qualitatively. Their effect is that the ideal dispersions $E_{\text{MR}}(k)$ and $E_{\text{SW}}(k)$ become multiplied by a nearly k -independent coefficient. The limiting values for $k \rightarrow \infty$ are reduced, both for nonzero thickness and LL mixing (Fig. 6). Since the SW energies in Coulomb units vary only slowly with B and β , the energies calculated at $B=5$ T and its corresponding $\beta=0.3$ [Eq. (5)] can be taken as representative for most of our experimental data. Exceptions for higher values of B will be explicitly mentioned.

Our best estimate of $E_{\text{SW}}(k \rightarrow \infty)$ starts with the torus [Table II column (a)]. Finite thickness ($\beta=0.3$) reduces this energy by about 10% [columns (b) and (d)], and so does the LL mixing at $B=5$ T [column (e)]. Combination of these two effects gives $E_{\text{SW}}(k \rightarrow \infty) \approx 0.035e^2/(4\pi\varepsilon\ell_0)$. As we argued at the end of Sec. III A and in Fig. 5, we believe this value would not change in a larger system and the $1/N \rightarrow 0$ extrapolation can be omitted. Note that with increasing magnetic field, β of the heterojunction increases, Eq. (5), while the LL mixing becomes less important. Quantitatively, the latter effect is stronger so that the indicated value of $E_{\text{SW}}(k \rightarrow \infty)$ in Coulomb units will very slightly increase with increasing magnetic field (cf. Fig. 6). In the case of $E_{\text{MR}}(k \rightarrow \infty)$ and the magnetoroton minimum, the LL mixing is found to have a minimal influence on the resulting energies [column (e) in Table II]. The finite thickness is then the main effect leading to the best-guess energies, 0.078 and 0.052, respectively.

TABLE II. Energies in $e^2/(4\pi\epsilon\ell_0)$ extracted from Fig. 6 (SW, MR, MR min) and Fig. 7 [Sky(1), ASky(1), QE]. The “best guess” is the torus value for $\beta=0.3$ and $B=5$ T (SW, MR, MR min) and it is the value from the sphere with $\beta=0.3$, $B=5$ T extrapolated to $1/N \rightarrow 0$ (Sky, ASky). For the QE we used $\beta=0.35$ and $B=15$ T together with the extrapolation $1/N \rightarrow 0$.

	Torus		Sphere				Best guess
	(a)	(b)	(c)	(d)	(e)	(f)	
	Ideal	Finite width $\beta=0.3$	Ideal	Finite width $\beta=0.3$	+LL mixing $B=5$ T	$\beta=0.3$ + $1/N \rightarrow 0$	
SW	0.045	0.039	0.057	0.052	0.047		0.035
MR	0.093	0.080	0.102	0.089	0.087		0.078
MR min	0.063	0.054	0.076	0.069	0.067		0.052
Sky(1)			-0.0062	-0.0056	-0.0065	-0.0050	-0.0058
ASky(1)			-0.0112	-0.0102	-0.0118	-0.0088	-0.0102
QE			0.0385	0.0335	0.0424	0.0222	0.0240

The skyrmion and anti-skyrmion spectra at $\nu=\frac{1}{3}$ have been introduced in Fig. 3. Given the magnetic fields of our experiment, only the smallest (anti-)skyrmions, Sky(1) and ASky(1), may be relevant (Fig. 4). Contrary to the spin wave, their condensation energies relative to a bare QEr and QH, show a slight dependence on the system size (Fig. 7). A linear fit in $1/N$ leads to (anti-)skyrmion energies about 10% lower at $1/N \rightarrow 0$ than they are for $N=7$ [Table II, columns (d) and (f)]. In contrast, the QE energy becomes reduced by as much as 35%.

The finite thickness ($\beta=0.3$) also reduces the Sky(1), ASky(1), and QE energies by about 10%, 10%, and 15%, respectively [Fig. 8 and Table II, column (d)]. On the other hand, the Landau level mixing (second order, $B=5$ T) increases these energies by 15%, 15%, and 25%, respectively [Table II, column (e)]. These two effects together with the $1/N \rightarrow 0$ extrapolation lead to our best guesses for the energies relevant in our experiment: -0.0058 for Sky(1) and -0.0102 for ASky(1) for $B=5$ T and corresponding $\beta=0.3$. For a QE we obtain 0.0280 through the same procedure. All these energies will definitely be reduced when magnetic field is swept up because both LL mixing and finite thickness have this tendency. For instance at $B=15$ T and corresponding $\beta=0.35$, the QE energy is only 0.0240.

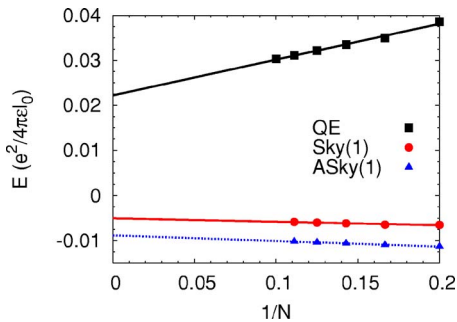


FIG. 7. (Color online) Extrapolation of the (anti-)skyrmion and QE energies to the thermodynamical limit $1/N \rightarrow 0$. Sphere, no LL mixing, finite width $\beta=0.33$.

IV. INTERPRETATION OF THE EXPERIMENTAL DATA

Our analysis of measured gaps, $\Delta(B)$, begins with a general observation that the gap can change either proportional to B (Zeeman energy) or proportional to \sqrt{B} (Coulomb energy)

$$\Delta[K] = E_C 50.2 \sqrt{B(\text{T})} + \Delta(S_z/\hbar) 0.295 [B(\text{T})] - E_d. \quad (6)$$

Here the Coulomb energy E_C should be put in units of $e^2/(4\pi\epsilon\ell_0)$ and $\Delta(S_z/\hbar)$ means the number of spins flipped in the excitation. Except for the disorder term, this equation is exact:⁴⁵ the energy difference between any two eigenstates of the Hamiltonian (1) at fixed ν scales²³ proportionally to $1/\ell_0 \propto \sqrt{B}$. If $\Delta S_z \neq 0$, a term proportional to B must be simply added since S_z is a good quantum number. Naturally, E_C and ΔS_z can be different for different excitations, introducing kinks into $\Delta(B)$. Between the kinks, however, $\Delta(B)$ should follow Eq. (6). With Landau level mixing and finite thickness taken into account, E_C in Eq. (6) becomes a function of B . However, these changes are very small in our range of mag-

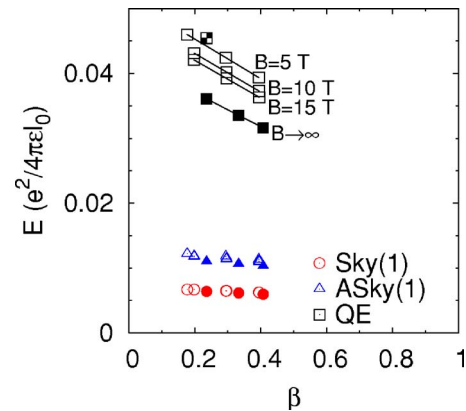


FIG. 8. (Color online) Analogous to Fig. 6 but for the QE energy relative to the energy of the QEr as well as for energies of the smallest skyrmion and anti-skyrmion. All data were obtained on a sphere, solid symbols refer to energies under no LL mixing.

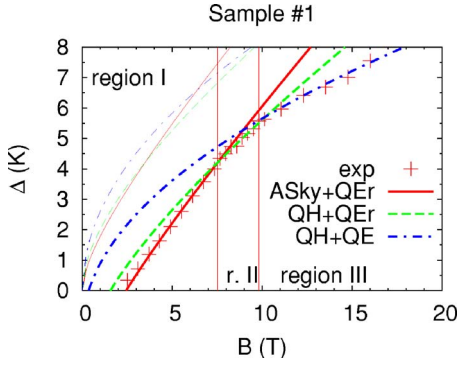


FIG. 9. (Color online) Gap energies of the sample 1 (Fig. 2) interpreted as an anti-skyrmion plus QEr for low B (region I) and a QE-QH pair for high B (region III). The disorder-induced gap reduction (E_d) obtained by fitting is 2.8, 2.3, and 1.4 K for regions I, II, and III, respectively. Thin lines correspond to $E_d=0$ and no fitting.

netic fields (cf. Sec. III C) so that E_C can be considered constant with a sufficient precision in the following analysis.

The reader may allow a short digression here: if we wish to have a fit-free model and neglect the disorder [$E_d=0$ in Eq. (6)], the energies calculated in the previous section and plugged into Eq. (6) can still qualitatively explain the experiments, as indicated by the thin lines in Fig. 9. In particular, we find that the gap is determined by more than one excitation across the range of magnetic fields in Fig. 9.

Including the disorder effects, the general line of the analysis for each single excitation is the following: (i) determine $\Delta(S_z/\hbar)$, (ii) obtain E_C , E_d by least-squares fitting, and (iii) compare E_C to the exact diagonalization. It should be noted that it is also possible to completely avoid the fitting procedure if the disorder is neglected. Energies calculated in Sec. III can be directly put into Eq. (6) (with $E_d=0$) and the obtained gap $\Delta(B)$ gives qualitatively the same result as observed experimentally (Fig. 2). Nevertheless, such calculated gaps are by ≈ 2 K too large and also the values of the magnetic field at transitions between different excitations are shifted. Since we aim at a quantitative understanding of the gaps seen in experiments where disorder is ever present we will use the former method.

The B dependence of the activation gap in the sample 1 shows an apparent transition slightly below 10 T. Let us divide the investigated range of magnetic field into three regions as depicted in Fig. 9: I (low field), II (transition), and III (high field).

In the following we wish to argue that the lowest excitation which determines the activation gap in region I is a QEr-anti-skyrmion ($K_A=1$) pair. In region III, QE-QH pairs without spin flip are observed while the QEr-QH pairs likely show up in region II.

The experimental data in region I, Fig. 9, show a remarkably precise linear behavior. Within the uncertainty of the measurement, this linearity does not necessarily mean that the Coulomb contribution to the gap entirely vanishes, but it sets a rather stringent upper limit of approximately $E_C < 0.025$. The choices $\Delta(S_z/\hbar)=0$ or 1 would lead to E_C larger than that (0.068 and 0.045); in other words if any of

these choices had been correct, $\Delta(B)$ would have exhibited a significant curvature in region I. On the other hand, $\Delta(S_z/\hbar) \geq 3$ leads to $E_C < 0$ and there is no support for such excitations in the theory. Even though skyrmion condensation energies are negative, the positive QEr-QH energy is always larger. The last option, $\Delta(S_z/\hbar)=2$, leads to $E_C=0.021$ and $E_d=2.8$ K. There are three possibilities for an excitation with two spin flips: ASky(2)+QE, ASky(1)+QEr, QH+Sky(1). However, quasielectrons are likely to be relevant first at higher magnetic fields (beyond 10 T) and skyrmions at quite small magnetic fields (around 1 T). Therefore, in this case, the most likely pair of charged particles created by a thermal excitation will be a QEr-ASky ($K_A=1$). The energy cost of this excitation, two spin flips plus Coulomb energy $E_C \approx 0.035 - 0.011 = 0.024$ (Sec. III C), is in nice agreement with the value mentioned above.

As the magnetic field increases, the $K_A=1$ anti-skyrmion becomes more energetically costly than a plain quasihole (Fig. 4). The gap should then amount to creation of a QH-QEr pair, i.e., to one spin flip plus $E_C \approx 0.035$. Taking $\Delta(S_z/\hbar)=1$ and focusing on region II, we obtain by fitting $E_C=0.033$ and $E_d=2.3$ K. However, as region II is not very large (Fig. 9), it might be that we observe in fact just a smooth transition between regions I and III.

Finally, for yet higher magnetic fields, it is more favorable to create a quasielectron in a higher CF LL than to flip its spin (QE preferred over QEr; Fig. 4, above). In line with the situation of the $B \rightarrow \infty$ limit, we expect a QH-QE pair to be the lowest excitation. Indeed, assuming $\Delta(S_z/\hbar) > 0$ in region III leads to negative E_d and unrealistic E_C with no justification in the calculated spectra. On the other hand, $\Delta(S_z/\hbar)=0$ gives $E_C \approx 0.045$ and $E_d=1.5$ K.

The last mentioned Coulomb energy is almost by a factor of 2 smaller than $E_{MR}(k \rightarrow \infty)$ from the exact diagonalization (Fig. 6 and Table II). However, it is remarkable how close the value $E_C \approx 0.045$ lies to the energy of the magnetoroton minimum. It is then tempting to conclude that the activation process goes in this case in two steps, creation of a magnetoroton and unbinding of the constituent QE and QH. The former step costs more energy, roughly $E_{MR}(1.4\ell_0^{-1}) = 0.05E_{MR}(k \rightarrow \infty) - E_{MR}(1.4\ell_0^{-1}) = 0.08 - 0.05 = 0.03$ for the unbinding of a magnetoroton (cf. Table II). The creation is therefore a bottleneck for the whole activation process and it determines the activation energy measured in transport in the limit of high Zeeman energies. Such a two-step process is not possible for the spin-flip excitations because the spin wave dispersion has no minimum which could lead to a stable intermediate state. We wish to stress that the activation gap smaller than the theoretical predictions of $E_{MR}(k \rightarrow \infty)$ has been observed many times^{43,46,47} but the problem was never conclusively resolved. Usually, this discrepancy was as a whole attributed to the disorder. Here we propose that the smaller observed gap for no-spin-flip excitations is only in part due to the disorder. For the sample 1, this B -independent reduction is $E_d \approx 1.4$ K. The other, “traditional,” interpretation that the disorder reduces the Coulomb energy, meaning $E_d=0$ and a modified value of E_C in (6), is in conflict with the gaps observed in region I (Fig. 9), which obviously do not extrapolate to $\Delta=0$ at $B=0$. It should be noted that we

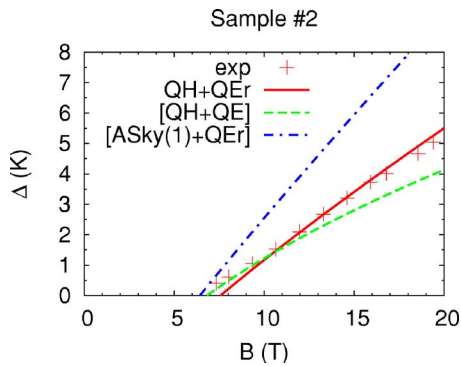


FIG. 10. (Color online) Gap energies of the sample 2 (Fig. 2) interpreted as a spin wave (a QH-QEr pair). The gap reduction 5.5 K is larger than for the sample 1. For other options [two spin flips=ASky(1)+QEr and zero spin flips=QE+QH], the parameters were taken as in Fig. 9; only the constant offset E_d was adjusted.

indeed found different gap reductions for different excitations within the same sample (Fig. 9). An attempt to take the value of $E_d=2.8$ K related to ASky(1)+QEr (region I) and use it also for region III leads to only a slightly changed E_C while the quality of the fit is worse.

The data of sample 2 suggest that we measure a single excitation in the whole range of accessible magnetic fields (Fig. 10). Again, we point out the striking linearity of $\Delta(B)$. When identifying the probed excitation, other choices than $\Delta(S_z/\hbar)=1$ lead to apparently wrong fits. Compared to the experimental data they either lead to a steeper $\Delta(B)$ even for zero E_C or diverge too much from the linear behavior (dash-dotted and dashed lines in Fig. 10). The only feasible excitation with $\Delta(S_z/\hbar)=1$ is a spin wave (QEr-QH pair). The calculated energy of a spin wave is somewhat larger than what the experimental data suggest ($E_C \approx 0.025$ with $E_d = 5.5$ K) and the most likely reason for this discrepancy is the disorder of the sample which is too strong to be described by a single parameter E_d .

The absence of skyrmionic excitations for sample 2 is not surprising given its lower mobility. The lower quality means a larger disorder-induced gap reduction ($E_d \approx 6$ K) implying a higher FQHE threshold in B ($B \gtrsim 7$ T) (cf. Figs. 10 and 9). These are too high fields for (anti-)skyrmions to be observed (Fig. 4). Less obvious is the absence of a transition to a spinless excitation (QE+QH) like the one observed for sample 1. We find, however, that such an excitation would be observable below 20 T only if E_d for QE+QH were above 5 K. By comparison with typical gap reductions in sample 1 this seems unlikely.

The present measurements suggest that, paradoxically, single spin-flip excitations may be observed up to rather high magnetic fields (20 T) even in samples with mobility below $100 \text{ m}^2/\text{V s}$. However, in order to observe larger

(anti-)skyrmions in FQH systems the Zeeman energy should be suppressed.^{26,48} By applying the hydrostatic pressure and reducing the Landé g factor, the maximum of three spin flips per excitation was reached¹⁹ compared to two spin flips of our experiment. In an ideal case, one should be able to observe more transitions in $\Delta(B)$, not just one as in Fig. 9, corresponding to successive reduction of skyrmion and anti-skyrmion sizes with increasing magnetic field (or Zeeman energy) at fixed filling factor.

V. CONCLUSION

Spin excitations in the $\nu=1/3$ FQH system were studied using measurements of the activation gap Δ as a function of magnetic field. Supported by energies obtained by exact diagonalization we identified the activation-relevant excitation to be a spin wave in the sample 2 and an anti-skyrmion with one spin flip plus a quasielectron with reversed spin for the sample 1. The abrupt change in $\Delta(B)$ observed at $B \approx 9$ T in the sample 1 was attributed to the transition to a charge density wave in the lowest excitation. Since the gap was in this case smaller than what we would expect for a charge density wave with infinite wave vector, we proposed that the activation is a two-step process with magnetoroton minimum governing the activation energy as a bottleneck. With this interpretation, we found the effect of disorder to be a constant reduction E_d of the gap, independent of magnetic field, in agreement with previous works.^{21,22} Consistent with its lower mobility, the gap reduction is larger for sample 2 and it is different for different types of excitations.

In order to obtain a quantitative agreement between the energies from the exact diagonalization and the experiment, the finite thickness as well as the Landau level mixing up to the first order have to be included. We wish to stress that the number of spin flips involved in the particular excitations can be determined with very high certainty even with little knowledge of the Coulomb energy. This is on one hand owing to the precision of the experimental data showing linear $\Delta(B)$ and on the other hand because the number of spin flips should be an integer. Our only fitting parameter was the constant disorder-induced reduction of the activation gap.

ACKNOWLEDGMENTS

It is our pleasure to thank Milan Orlita for careful reading of the manuscript and Eros Mariani and Daniela Pfannkuche for worthwhile discussions. A.D. and R.H. acknowledge support via the DFG priority program ‘‘Quanten Hall Systeme’’ and BMBF; A.W. acknowledges support from Grant No. 2P03B02424 of the Polish MENiS; and K.V. and O.Č. acknowledge support by the Academy of Sciences of the Czech Republic under Institutional Support No. AV0Z10100521 and by the Ministry of Education of the Czech Republic Center for Fundamental Research LC510.

- *Centre for Atom Optics and Ultrafast Spectroscopy, Faculty of Engineering and Industrial Science, Swinburne University of Technology, Mail H38, PO Box 218, Hawthorn, VIC 3122, Australia
- ¹S. E. Barrett, G. Dabbagh, L. N. Pfeiffer, K. W. West, and R. Tycko, *Phys. Rev. Lett.* **74**, 5112 (1995).
 - ²A. Schmeller, J. P. Eisenstein, L. N. Pfeiffer, and K. West, *Phys. Rev. Lett.* **75**, 4290 (1995).
 - ³E. H. Aifer, B. B. Goldberg, and D. A. Broido, *Phys. Rev. Lett.* **76**, 680 (1996).
 - ⁴D. K. Maude, M. Potemski, J. C. Portal, M. Henini, L. Eaves, G. Hill, and M. A. Pate, *Phys. Rev. Lett.* **77**, 4604 (1996).
 - ⁵*Composite Fermions*, edited by O. Heinonen (World Scientific, Singapore, 1998).
 - ⁶H. A. Fertig, L. Brey, R. Côté, and A. H. MacDonald, *Phys. Rev. B* **50**, 11018 (1994).
 - ⁷S. L. Sondhi, A. Karlhede, S. A. Kivelson, and E. H. Rezayi, *Phys. Rev. B* **47**, 16419 (1993).
 - ⁸D. H. Lee and C. L. Kane, *Phys. Rev. Lett.* **64**, 1313 (1990).
 - ⁹K. Moon, H. Mori, K. Yang, S. M. Girvin, A. H. MacDonald, L. Zheng, D. Yoshioka, and S.-C. Zhang, *Phys. Rev. B* **51**, 5138 (1995).
 - ¹⁰X. C. Xie and S. He, *Phys. Rev. B* **53**, 1046 (1996).
 - ¹¹A. Wójs and J. J. Quinn, *Phys. Rev. B* **66**, 045323 (2002).
 - ¹²E. H. Rezayi, *Phys. Rev. B* **43**, 5944 (1991).
 - ¹³E. H. Rezayi, *Phys. Rev. B* **56**, R7104 (1997).
 - ¹⁴X.-G. Wu and S. L. Sondhi, *Phys. Rev. B* **51**, 14725 (1995).
 - ¹⁵E. H. Rezayi, *Phys. Rev. B* **36**, 5454 (1987).
 - ¹⁶R. Kamilla, X. Wu, and J. Jain, *Surf. Sci.* **99**, 289 (1996).
 - ¹⁷A. H. MacDonald and J. J. Palacios, *Phys. Rev. B* **58**, R10171 (1998).
 - ¹⁸T. Chakraborty and P. Pietiläinen, *Phys. Rev. Lett.* **76**, 4018 (1996).
 - ¹⁹D. R. Leadley, R. J. Nicholas, D. K. Maude, A. N. Utjuzh, J. C. Portal, J. J. Harris, and C. T. Foxon, *Phys. Rev. Lett.* **79**, 4246 (1997).
 - ²⁰P. Khandelwal, N. N. Kuzma, S. E. Barrett, L. N. Pfeiffer, and K. W. West, *Phys. Rev. Lett.* **81**, 673 (1998).
 - ²¹R. Morf and N. d'Ambrumenil, *Phys. Rev. B* **68**, 113309 (2003).
 - ²²A. F. Dethlefsen, E. Mariani, H.-P. Tranitz, W. Wegscheider, and R. J. Haug, *Phys. Rev. B* **74**, 165325 (2006).
 - ²³T. Chakraborty and P. Pietiläinen, *The Quantum Hall Effects*, 2nd ed. (Springer, Berlin, 1995).
 - ²⁴D. Yoshioka, *The Quantum Hall Effect* (Springer, Berlin, 2002).
 - ²⁵F. D. M. Haldane, *Phys. Rev. Lett.* **51**, 605 (1983).
 - ²⁶D. Yoshioka, B. I. Halperin, and P. A. Lee, *Phys. Rev. Lett.* **50**, 1219 (1983); D. Yoshioka, *Phys. Rev. B* **29**, 6833 (1984).
 - ²⁷F. D. M. Haldane and E. H. Rezayi, *Phys. Rev. B* **31**, R2529 (1985).
 - ²⁸C. Nayak and F. Wilczek, *Nucl. Phys. B* **455**, 493 (1995).
 - ²⁹T. Chakraborty, *Surf. Sci.* **229**, 16 (1990).
 - ³⁰T. Chakraborty and P. Pietiläinen, *Phys. Rev. B* **41**, 10862 (1990).
 - ³¹R. B. Laughlin, *Phys. Rev. Lett.* **50**, 1395 (1983).
 - ³²A. Wójs and J. J. Quinn, *Phys. Rev. B* **61**, 2846 (2000).
 - ³³S.-Y. Lee, V. W. Scarola, and J. K. Jain, *Phys. Rev. B* **66**, 085336 (2002).
 - ³⁴T. Chakraborty, P. Pietiläinen, and R. Shankar, *Europhys. Lett.* **38**, 141 (1997).
 - ³⁵S. M. Girvin, A. H. MacDonald, P. M. Platzman, *Phys. Rev. B* **33**, 2481 (1986).
 - ³⁶G. Murthy, *Phys. Rev. B* **60**, 13702 (1999).
 - ³⁷A. H. MacDonald and G. C. Aers, *Phys. Rev. B* **29**, 5976 (1984).
 - ³⁸F. C. Zhang and S. Das Sarma, *Phys. Rev. B* **33**, 2903 (1986).
 - ³⁹T. Ando, A. Fowler, and F. Stern, *Rev. Mod. Phys.* **54**, 437 (1982).
 - ⁴⁰R. H. Morf, N. d'Ambrumenil, and S. Das Sarma, *Phys. Rev. B* **66**, 075408 (2002).
 - ⁴¹D. Yoshioka, *J. Phys. Soc. Jpn.* **55**, 885 (1986).
 - ⁴²K. Výborný, Ph. D. thesis, Universität Hamburg 2005, www.sub.uni-hamburg.de/opus/volltexte/2005/2553
 - ⁴³R. L. Willett, H. L. Stormer, D. C. Tsui, A. C. Gossard, and J. H. English, *Phys. Rev. B* **37**, 8476 (1988).
 - ⁴⁴A. H. MacDonald, K. L. Liu, S. M. Girvin, and P. M. Platzman, *Phys. Rev. B* **33**, 4014 (1986).
 - ⁴⁵Equation (6) strictly follows from the exact Hamiltonian (1) under three assumptions: (a) we stay in a region of parameters where the ground state and the probed excitation stay always the same, (b) we accept the presented model of the disorder (Sec. III B), and (c) either the system is ideal (no LL mixing, zero thickness) or the corresponding parameters change only a little. The validity of (c) follows from Figs. 6 and 8. Ranges of B where (a) holds either can be found from the energies theoretically calculated in Sec. III C if $E_d=0$ or they can be identified by apparent kinks in the experimental data for $\Delta(B)$ when disorder is not neglected.
 - ⁴⁶G. S. Boebinger, A. M. Chang, H. L. Stormer, and D. C. Tsui, *Phys. Rev. Lett.* **55**, 1606 (1985).
 - ⁴⁷G. S. Boebinger, H. L. Stormer, D. C. Tsui, A. M. Chang, J. C. M. Hwang, A. Y. Cho, C. W. Tu, and G. Weimann, *Phys. Rev. B* **36**, 7919 (1987).
 - ⁴⁸I. V. Kukushkin, K. von Klitzing, and K. Eberl, *Phys. Rev. B* **60**, 2554 (1999).